

See discussions, stats, and author profiles for this publication at: <https://www.researchgate.net/publication/231376930>

Nanosilica Addition Dramatically Improves the Cell Morphology and Expansion Ratio of Polypropylene Heterophasic Copolymer Foams Blown in Continuous Extrusion

ARTICLE *in* INDUSTRIAL & ENGINEERING CHEMISTRY RESEARCH · MAY 2011

Impact Factor: 2.59 · DOI: 10.1021/ie102438p

CITATIONS

31

READS

77

3 AUTHORS, INCLUDING:



Wentao Zhai

Chinese Academy of Sciences

62 PUBLICATIONS 978 CITATIONS

SEE PROFILE



C.B. Park

University of Toronto

540 PUBLICATIONS 7,004 CITATIONS

SEE PROFILE

Nanosilica Addition Dramatically Improves the Cell Morphology and Expansion Ratio of Polypropylene Heterophasic Copolymer Foams Blown in Continuous Extrusion

Wentao Zhai,^{†,‡} Chul B. Park,^{‡,*} and Marianna Kontopoulou[§]

[†]Ningbo Institute of Material Technology and Engineering (NIMTE), Chinese Academy of Sciences, Ningbo, Zhejiang province, 315201, China

[‡]Microcellular Plastics Manufacturing Laboratory, Department of Mechanical and Industrial Engineering, University of Toronto, Toronto, Ontario, M5S 3G8

[§]Department of Chemical Engineering, Queen's University, Kingston, ON K7L3N6, Canada

ABSTRACT: Currently, the preparation of polypropylene (PP) foam with a well-defined cell structure and a high expansion ratio is receiving increased attention. However, the present technical problems such as poor cell nucleation ability and weak melt strength of polymer resin, hinder the broader use of linear PP in foam production. In this study, a PP heterophasic copolymer with a linear structure was selected together with nanosilica to challenge the fabrication of PP foam with uniform cell structure, high cell density, and a high expansion ratio using CO₂ as a physical blowing agent. Scanning electron microscopy (SEM) observation indicated that silica particles tended to aggregate in the PP matrix, but the multisilica aggregates with sizes from 80 to 350 nm were well dispersed in PP because of the addition of a coupling agent (CA). PP foam exhibited poor cell morphology and low cell densities of ca. 10^{4–5} cells/cm³ at different die temperatures. An introduction of a small amount of nanosilica, 0.5 wt % and 1 wt %, dramatically improved the foaming behavior of PP, where the cell structure distribution of the resultant foams was uniform, and the cell density and foam expansion were high (i.e., 10^{8–9} cells/cm³ and 16.9–19.5, respectively). Furthermore, the presence of nanosilica clearly broadened the foaming window of PP. By further increasing silica content, however, the foaming behavior of PP/silica nanocomposites became poor, especially at slightly higher die temperatures (i.e., above 140 °C), even though a high silica loading increased the number of heterogeneous nucleation sites. The effect of foaming on the dispersion of nanosilica in the PP matrix was also investigated.

INTRODUCTION

Considerable efforts have recently been dedicated to the development of polypropylene (PP) foams as substitutes for conventional polystyrene and polyethylene foams. Such studies have been motivated by the need to increase the service temperature and material properties of PP foams to broaden their applications. However, researchers have found that linear PP resin's foamability is usually poor due to its weak melt strength and melt elasticity, which cause high open-cell content and nonuniform cell distribution in the final foamed samples.^{1–3} Some companies have developed high melt strength PP (HMSPP) resins in an effort to produce PP foams with a fine cell structure and high foam expansion. But there are financial challenges to the wide use of HMSPP resin, as it costs at least twice as much as conventional PP.

The addition of nanofillers has been considered an effective way to improve the foamability of PP. It has been found that the presence of nanofillers with a high L/D ratio can increase melt strength and induce strain hardening in the low-melt-strength polymers.^{4–7} It is known that cell growth is extensional flow of the polymer/gas solution in nature and the biaxial stretching of cell walls during the polymeric foaming process.⁸ At the same time, the increased melt strength that results from nanofiller addition is expected to stabilize cell structure and to, therefore, suppress cell coalescence. This hypothesis has been verified by the alignment of nanoclay particles in a cell wall with TEM

observation and the improved cell morphology during PP batch foaming.⁹ In a study of extrusion foaming, Zheng et al.¹⁰ verified that the introduction of nanoclay led to the formation of microcellular PP, which was the result of enhanced cell nucleation. Using the same foaming method, we found that adding nanoclay clearly broadened the suitable foaming window of PP,¹¹ and increased the cell density from 10^{3–4} to 10⁸ cells/cm³ and expansion ratio from 1.7 to 2.2 to 18.8.

The main requirements for PP resins in foam fabrication are believed to be the presence of a broad foaming window, and the formation of both a fine cell structure and high foam expansion. As seen in previous studies,^{10,11} however, PP homopolymer nanocomposites normally exhibit a narrow foaming window and a high foam expansion could only be achieved at a low die temperature, while HMSPP had a quite broad foaming window.^{12,13} Lee et al.¹⁴ investigated the foaming behavior of PP copolymer by using butane as a physical blowing agent, and found that heterophasic PP copolymer had a broad foaming window, and a high foam expansion could be achieved even at a high die temperature. One limitation of pure PP foaming is its low cell density, which results from poor cell nucleation.¹⁴ It is

Received: December 4, 2010

Accepted: May 10, 2011

Revised: May 7, 2011

Published: May 10, 2011

Table 1. Characterizations of PPCA and PPS Nanocomposites

CA		SiO ₂		CA	T _m /	T _c /
samples	content/wt%	samples	content/wt%	content/wt%	°C	°C
		PP	0	0	166.7	126.7
PPCA-1	4.8	PPS0.5	0.5	4.8	166.1	126.8
PPCA-2	9.5	PPS1.0	1.0	9.5	165.9	126.3
PPCA-3	19.0	PPS2.0	2.0	19.0	166.0	126.4
PPCA-4	47.5	PPS5.0	5.0	47.5	165.8	126.8

expected that the introduction of nanoparticles would improve the cell nucleation behavior of PP, and that the potential increase in melt strength would suppress cell coalescence.¹¹ Therefore, PP/filler nanocomposites may provide us with an alternative to HMSPP that could produce good foamed samples.

In this study, a linear PP with a melt flow index of 3.5 g/10 min was selected. A PP/silica (PPS) nanocomposite master batch with a silica content of 5 wt % was prepared first using a twin-screw extruder, and then a series of composites with various silica contents were obtained by diluting the master batch with neat PP. SEM was used to characterize the dispersion of silica in the PP matrix. Using an extrusion method, PP and PPS nanocomposites were foamed with 5 wt % CO₂ as a physical blowing agent, and the foamed samples were obtained using high to low die temperatures. The cell morphology and expansion ratio of the foams in relation to the die temperature and nanosilica content were evaluated. A map for a suitable foaming window was then established. On the basis of the cell density and melt viscosity data, the mechanism of how silica introduction affected PP foaming behavior was studied from the perspective of cell nucleation and cell coalescence. Afterward, the effect of polymeric foaming on the dispersion of silica was examined.

EXPERIMENTAL SECTION

Materials. A PP, BC240TF, with a melt flow rate of 3.5 g/10 min was provided by Borealis. Maleic anhydride-grafted PP (PP-g-MA), Epolene G3003 with a melt flow index (MFI) of 360 g/10 min was used as a coupling agent (CA) with maleic anhydride (MA) level of 1.2%, according to the supplier. Silica, AEROSIL200, manufactured by Evonik, is a hydrophilic fumed silica with a specific surface area of 200 m²/g and an average primary particle size of 12 nm. CO₂ with a purity of 99.5% (Linde gas) was used as a physical blowing agent.

Nanocomposite Preparation. The PP, CA, and silica were vacuum-dried at 80 °C for 8 h before use. The PP was dry blended using the same amount of CA, and a PP/silica premix was prepared by dry blending the PP and CA mixtures with the silica. The premix was subsequently melt extruded using a counter-rotating twin-screw compounder by maintaining a temperature of 200 °C with a screw speed of 150 rpm. The silica content prepared for the master batch was 5 wt %. A series of nanocomposites with a clay content of 0.5, 1, 2, and 5 wt % was obtained by diluting the masterbatch with the PP and were thereafter coded as PPS0.5, PPS1.0, and PPS2.0, and PPS5.0, respectively. Considering the large amount of CA used in each composition, PP/CA blends were prepared in this study for comparison, which had the same CA loading with the corresponding PPS as shown in Table 1.

Extrusion Foaming. In our previous studies we described the single extrusion foaming system used in this experiment.² A filamentary die with an L/D 0.413"/0.051" was used for the foaming experiments. The CO₂ content injected into the barrel, which was fixed to 5 wt % throughout the experiment, was accurately adjusted and regulated by controlling both the gas flow rate of the syringe pump and the material feed rate. Under the strong shear action of screw mixing and the static mixers, a single-phase polymer solution resulted. When the polymer/gas solution entered the filament die, it experienced a rapid pressure drop, which caused a sudden decrease in gas solubility in the polymer. Hence a large number of bubbles were nucleated in the polymer matrix and a foam structure was created which was followed by bubble growth. The die temperature here was equivalent to the temperature of the die and the heat exchanger. The foamed samples at different die temperatures were collected for cell morphology observation and cell density measurement.

Characterizations. The melting peak (*T_m*) and crystallinity of the PP and PPS samples before and after foaming were determined by using a Q2000 DSC (TA Instruments) calibrated with indium. For all samples, the DSC heating and cooling rates of the DSC tests were fixed at 20 °C/min, and only data obtained from a second heating were recorded. The degree of crystallinity was calculated from the integration of the DSC melting peaks and by using 290 J/g as the heat of fusion of 100% crystallized PP.¹⁵

Dynamic rheological measurements were carried out on a strain-controlled ARES rheometer (TA Instruments), using 25 mm parallel-plate geometry and a 1 mm sample gap. Dynamic shear measurements were performed at frequencies from 0.01 to 70 rad/s at temperatures of 190 °C using strain values determined by a strain sweep to lie within the linear viscoelastic regions.

Two scanning electron microscopes (SEM), Hitachi S-5200 and JEOL JMS 6060, were used to observe the dispersion of silica in the PP matrix and the cell morphology of the foamed samples. The samples were freeze-fractured in liquid nitrogen and sputter-coated with platinum. Both cell size and density were determined from the SEM micrographs. The cell density (*N₀*), the number of cells per cubic centimeter of unfoamed polymer, was determined by eq 1:

$$N_0 = \left[n \frac{M^2}{A} \right]^{3/2} \phi \quad (1)$$

where *n* is the number of cells in the SEM micrograph, *M* is the magnification factor, *A* is the area of the micrograph (in cm²), and *φ* is the volume expansion ratio of the polymer foam, which can be calculated in accord with eq 2:

$$\phi = \frac{\rho}{\rho_f} \quad (2)$$

where *ρ* and *ρ_f* are the mass densities of samples before and after foaming, respectively, which were measured via the water displacement method in accord with ASTM D792.

RESULTS AND DISCUSSION

Dispersion of Silica in the PP Matrix. PPS nanocomposite master batch with a silica content of 5 wt % was produced by a twin-screw extruder. To improve the favorable PP-silica interactions, 47.5 wt % PP-g-MA was used as a CA. A series of PPS nanocomposite samples with low silica content were obtained by

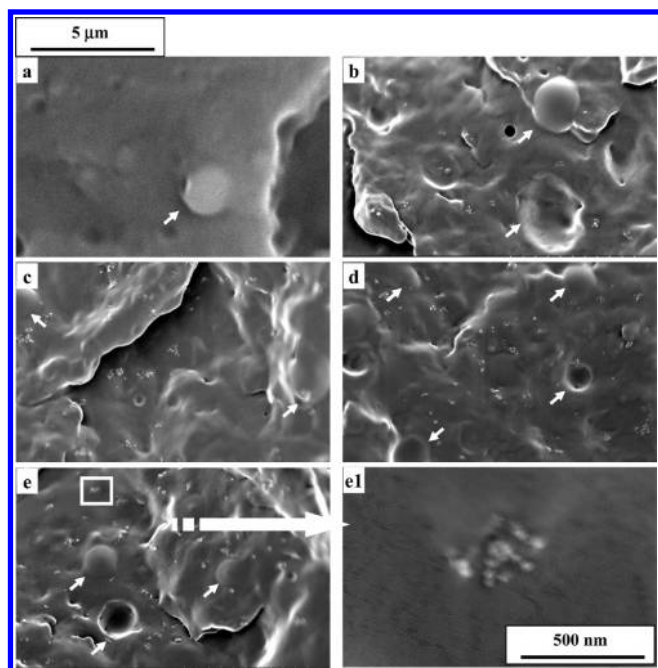


Figure 1. Dispersion of silica in PP matrix: (a) PP; (b) PPS0.5; (c) PPS1.0; (d) PPS2.0; (e, e1) PPS5.0. The brighter irregular shaped particles are multisilica aggregates, and the spherical particles pointed by arrows are phase-separated rubber phase or CA phase.

diluting the batch with pure PP. Figure 1 shows SEM micrographs of the resultant PP and PPS nanocomposites with different silica content. The brighter irregularly shaped particles in the PP matrix are multisilica aggregates with a size of about 80–350 nm. It is clear that PPS5.0 has plentiful well-dispersed multisilica aggregates after melt compounding. The SEM micrograph with high magnification, as shown in Figure 1(d1), indicates that each aggregate includes dozens of silica particles. By decreasing the silica content of the masterbatch, the number of aggregates was reduced while the size and dispersion of the aggregates by the dilution processing did not change significantly. This demonstrated that the aggregates in the masterbatch were not obviously redispersed or further aggregated by dilution processing.

The hydrophilic fumed silica has a large amount of hydroxyls on its surface. These surface hydroxyls increase the tendency of silica to create hydrogen bonds between nanoparticles and directly result in the formation of aggregates. These bonds are sufficiently powerful to keep the particles agglomerated, even during the compounding process, where powerful shear stresses are applied to the surfaces of the agglomerates. The MA group in CA is a rigid five-membered ring with a permanent dipole moment. The surface hydroxyl groups of the silica can react with the MA groups of the CA, leading to the formation of chemical bonding between the silica and the CA, resulting in improved compatibility between the PP and the silica.¹⁶ Also, due to silica's very large surface area, it had been expected that the stress applied during the melt compounding process would easily transfer from the matrix onto the silica particles.¹⁷ These interactions facilitated an increase in the degree of silica dispersion in the PP matrix. Therefore, although the melt processing was by itself ineffective in dispersing the silica individually in the PP, the addition of CA improved its

interaction with the polymer, and reduced the size of silica aggregates in PP.

The presence of spherical particles with the size about 1.5–3.0 μm were observed in the PP and PPS nanocomposite samples. These spherical particles exhibited poor compatibility with the PP matrix because of weak bonding at the interfaces. The presence of spherical holes possibly resulted from the fracture process. It is known that PP heterophasic copolymer is a blend of HPP and ethylene-propylene rubber (EPR) that can be introduced by postreactor or compounding. The EPR is not miscible in HPP matrix, which was verified with chemical etching in our previous study.¹⁴ Therefore, the spherical particles in the PP and PPS nanocomposites were taken to be EPR. On the other hand, a large amount of CA was used in this study to optimize the dispersion of silica in the PP matrix. It was reported that the MA content in PP-g-MA had an obvious effect on the miscibility of PP and CA, where a high MA content of 1.5 and 3.1% in PP-g-MA yielded a phase-separated morphology while PP-g-MA with a low MA content of 0.3% exhibited good miscibility with PP, where 20% CA was included in PP/CA blends.¹⁸ The PP-g-MA used in this study had a high MA content of 1.2%, which could induce phase separation between the PP and the CA, especially with a high CA content. This claim is further verified by SEM micrographs of the foamed PPS nanocomposite samples.

Addition of Silica Dramatically Improves Cell Morphology and Increases the Expansion Ratio of PP Foams. The preparation of foamed samples with fine cell structure and high expansion ratio is important because a well-defined cell morphology usually leads to improved foam properties. A high expansion ratio can also effectively reduce resin usage. PP and PPS nanocomposites were extrusion foamed using 5 wt % CO₂. The resulting cell morphologies are shown in Figure 2. As expected, PP foams exhibited poor cell morphology at high die temperatures of 140–145 °C, where the cell sizes were large. Decreased die temperature tended to slightly increase the cell morphology of PP foams, which was probably due to slightly increased melt strength at these temperatures. Even at lower temperature, the cell coalescence was still observed during PP extrusion foaming. The introduction of a small amount of silica dramatically improved the cell morphology of PPS foams. In the case of PPS0.5, well-defined cell morphologies (i.e., small cell size, high cell density, thin cell wall, and uniform cell distribution) were observed even at die temperatures of 145–140 °C. By further decreased die temperature to 135 °C, the cell morphology of the PPS0.5 foam continued to improve, where the cell sizes were smaller. With the silica content increased to 1.0 wt %, uniform cell distribution was observed in the PPS1.0 foams, and the lowest die temperature of 135 °C led to the best cell morphology. At a silica content of 2.0 wt %, cell morphologies were poor, where bigger cells and nonuniform cell distribution were seen at die temperatures of 145–140 °C. At 135 °C, however, the cell morphology became better. At a higher silica content of 5.0 wt %, the cell morphology of the PPS5.0 foams changed dramatically. At high die temperatures of 145–140 °C, the cell morphologies of PPS5.0 foam were poor and cell coalescence was obvious in the foam's core. At a lower die temperature of 130 °C, however, the foam's cell morphology tended to improve.

A foaming window is a useful way by which to evaluate the foamability of polymers. In general, a broad foaming window facilitates foam processing, while a narrow foaming window tends to make higher demands on the foaming system, particularly on the temperature control system. Figure 3 shows a suitable foaming

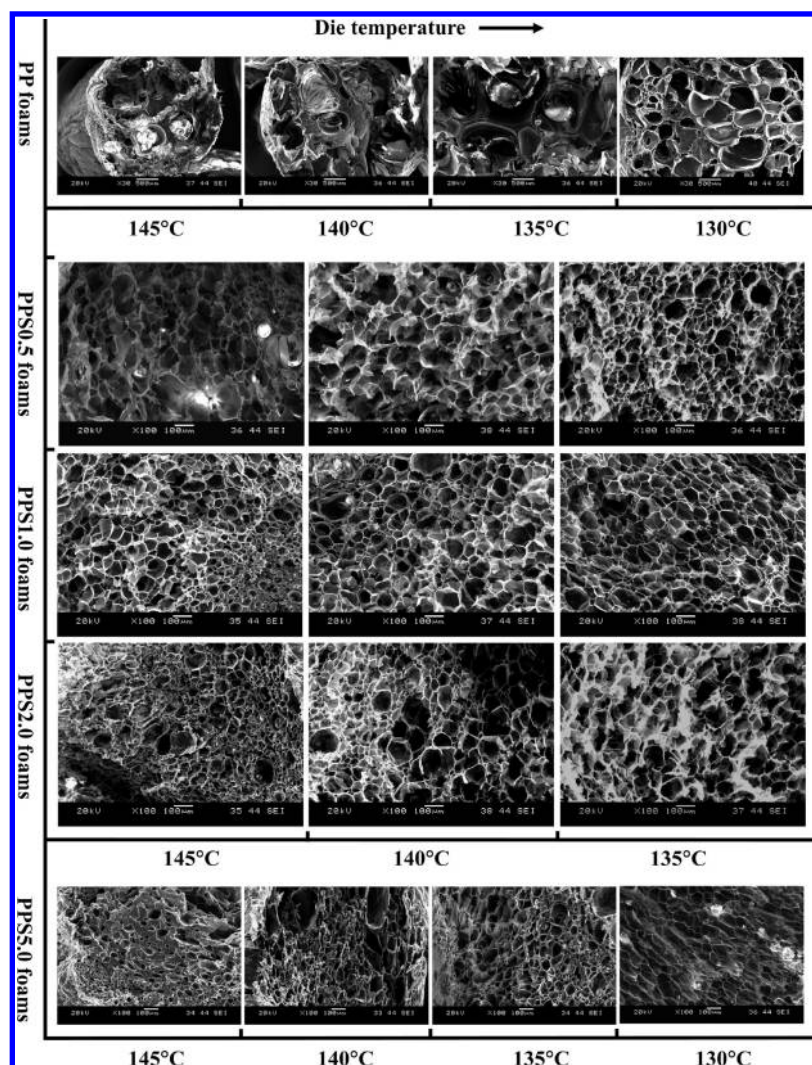


Figure 2. Cell morphology of PP and PPS nanocomposite foams obtained at different die temperatures.

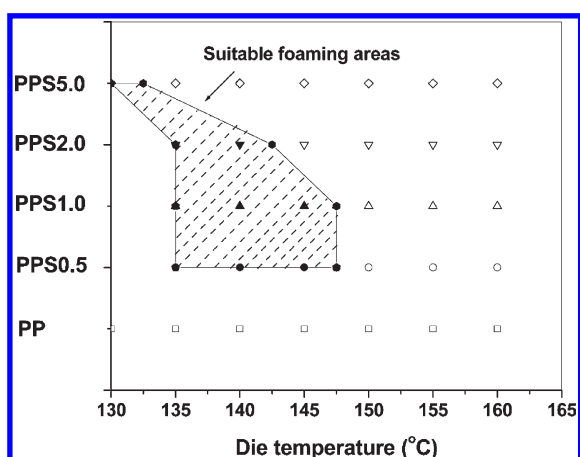


Figure 3. The suitable foaming window of PP and PPS nanocomposites blown with 5 wt % CO₂.

window for PP and PPS nanocomposites with respect to die temperature. The suitable foaming window in this figure means the foams obtained from those foaming regions had a well-defined cell structure with very thin walls and uniform cell distribution and

high expansion ratio; specifically, the cell density was higher than 10^7 cells/cm³ and the expansion ratio was higher than 8–10. In the case of pure PP, no suitable foaming window was found due to poor cell nucleation or the presence of cell coalescence. With the introduction of 0.5 and 1.0 wt % silica, PPS0.5 and PPS1.0 could produce good foamed samples at a die temperature of about 135–147.5 °C. This result indicated that the suitable foaming windows for PPS0.5 and PPS1.0 in this study were 12.5 °C. At a higher clay content of 2.0 and 5.0 wt %, however, narrower foaming windows of about 7.5 and 2.5 °C, respectively, offered good foamed samples. Therefore, the introduction of a small amount of silica dramatically improved the foamability of the PP.

The expansion ratio of PP and PPS nanocomposites at different die temperatures is shown in Figure 4. With PP, the resultant foams exhibited a low expansion ratio of about 2.5 at high die temperatures of 150–160 °C. With decreased die temperature, the expansion ratio of the PP increased gradually and further increased rapidly at die temperatures of 130–135 °C. The maximum expansion ratio of PP foam was 12.6, which was obtained at a die temperature of 130 °C. The introduction of a small amount of silica significantly increased the expansion ratio of PPS foams. For example, PPS0.5 foams had a much higher expansion ratio compared with PP foams, even at higher die

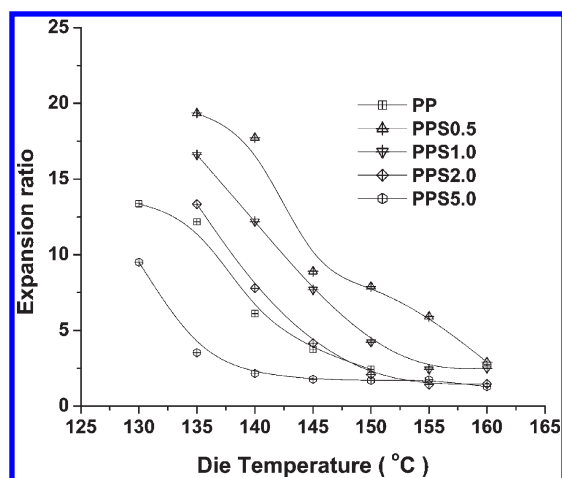


Figure 4. The expansion ratio of PP and PPS nanocomposites foams obtained at different die temperatures.

Table 2. Effect of Nanoparticle Addition on the Cell Density and Expansion Ratio of Polymers Foams

polymer nanocomposites	changing of cell density (cells/cm ³) ^a	changing of expansion ratio ^a
PP/silica ^b	10 ^{4–5} vs 10 ^{8–9}	2.2–12.9 vs 3.0–19.5 ^b
PP/clay ^{c11}	10 ^{3–5} vs 10 ^{7–8}	1.7–2.2 vs 1.7–18.8
PP/clay ^{d10}	10 ⁷ vs 10 ⁹	1.5–2.1 vs 2.3–7.0
crystalline PA/clay ^{e18}	10 ⁴ vs 10 ⁷	1.3 vs 1.6
HDPE/clay/WF ^{f19}	10 ⁶ vs 10 ^{7–8}	1.4–1.8 vs 1.5–1.8
mPE/clay/WF ^{g20}	10 ⁶ vs 10 ^{7–8}	1.2 vs 1.2–1.4

^a The former was the data of neat polymer, and the latter was that of polymer nanocomposites. ^b PP heterophasic copolymer: 1–5 wt % clay; 5 wt % CO₂ as physical blowing agent. ^c PP homopolymer: 1–5 wt % clay; 5 wt % CO₂ as physical blowing agent. ^d PP homopolymer: 1–5 wt % clay; 5 wt % CO₂ as physical blowing agent. ^e Crystalline nylon: 5 wt % clay; 5 wt % CO₂ as physical blowing agent. ^f High density polyethylene: 30 wt % wood fiber; 1 wt % clay; 0.3 wt % N₂ as physical blowing agent. ^g Metallocene polyethylene: 30 wt % wood fiber; 5 wt % clay; 1 wt % chemical blowing agent.

temperatures of 155–145 °C. At a lower die temperature of 135 °C, the expansion ratio of PPS0.5 foams was 19.5, which was much higher than the 12.1 of PP foams at the same temperature. By further increasing the silica content, however, PPS1.0 and PPS2.0 exhibited a gradually decreased expansion ratio at the foaming scopes, and the maximum expansion ratio obtained at 135 °C decreased from 19.5 for PPS0.5 to 16.9 for PPS1.0 and to 13.4 for PPS2.0. With a higher silica content, PPS5.0 foams showed a much lower expansion ratio at different die temperatures, that is, 2.1 at 160–140 °C and 9.8 at 130 °C, which was even lower in relation to the PP.

The addition of a small amount of nanoparticles has been reported to improve cell morphology and to increase the expansion ratio of continuously foamed nylon/clay,¹⁹ HDPE/WF/clay,²⁰ and mPE/WF/clay²¹ nanocomposites and even for polymers with low melt strength like PP/clay^{10,11} and poly(ether ether ketone)/carbon nanofibers⁷ nanocomposites. Compared with the previously reported materials in Table 2, however, the introduction of 0.5–1.0 wt % silica induced a much more obvious improvement in cell morphology and increase in foam expansion. The possible mechanism behind this phenomenon

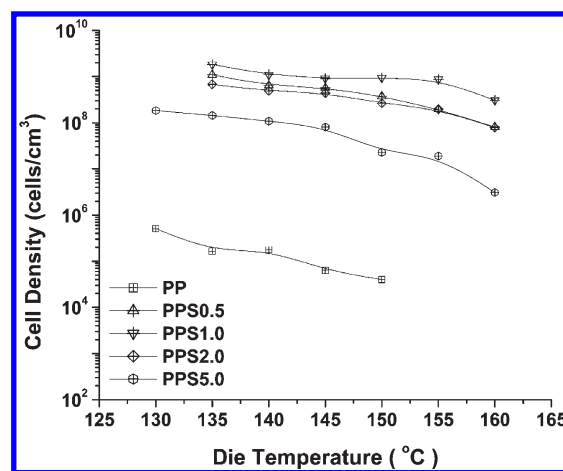


Figure 5. The cell density of PP and PPS nanocomposites foams obtained at different die temperatures.

will be explained in the following sections from the perspective of cell nucleation and coalescence.

Effect of Silica Addition on Cell Nucleation. Cell density is a value which shows the number of survived cells (per unfoamed unit volume) that undergo cell nucleation, cell collapse, and cell coalescence. It has been used by many researchers to investigate the cell nucleation process. Figure 5 shows the cell density of the PP and PPS nanocomposites at different die temperatures. The cell densities of PP foams were quite low, that is, 10^{4–5} cells/cm³, and the decreased die temperature slightly increased their cell density. With the introduction of 0.5 wt % silica, however, the cell densities of the PPS0.5 foams dramatically increased to 10^{7–8} cells/cm³ because cell nucleation was enhanced. By increasing the silica content further, the cell densities of the PPS1.0 and PPS2.0 foams gradually increased up to 10^{8–9} cells/cm³. For these PPS nanocomposite foams, a similar temperature dependence of cell density on die temperature was observed. At a higher silica content of 5 wt %, however, PPS5.0 foams exhibited an obvious reduced cell density of about 10^{7–8} cells/cm³. They also showed a higher temperature dependence of cell density on die temperature compared with the PPS0.5, PPS1.0, and PPS2.0 foams.

The increased cell density that occurs with the introduction of nanoparticles has been observed in various polymer/filler nanocomposite foaming systems. In general, the presence of nanoparticles in a polymer melt generally tends to decrease the energy barrier to cell nucleation based on the classical nucleation theory.²² A recent simulation study by Wang *et al.*²³ proved that the presence of fillers tends to induce a local stress variation around them in polymer/gas solutions, which dramatically increases the critical bubble radius, and hence increased the cell nucleation rate. The presence of a local stress variation was thought to be the main reason why the filler tended to decrease the energy barrier in cell nucleation. In another study, Wang *et al.* found that the cavities on fillers caused a distinct pressure fluctuation around the cavities.²⁴ This phenomenon suggested that the surface properties of fillers might also affect cell nucleation.^{25,26} In this study, silica had a high specific surface area (i.e., 200 m²/g), which was much higher than that of the other fillers, such as nanoclay, with surface areas of 13.1–173 m²/g.²⁷ In addition, multisilica aggregates were well dispersed in the PP matrix due to the introduction of CA. These attributes ensured that the silica could supply a large number of

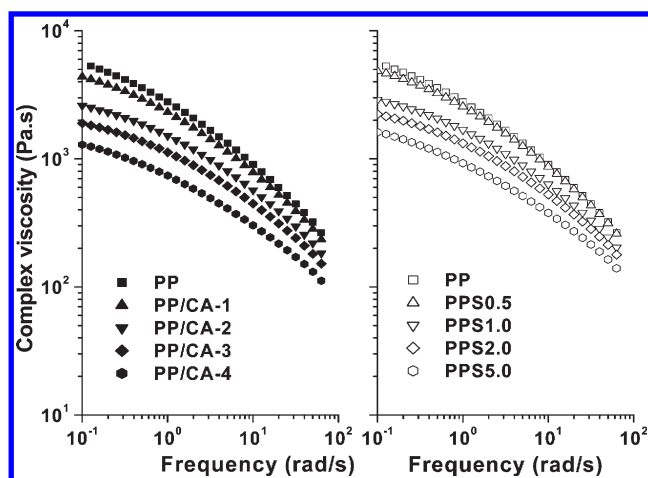


Figure 6. The complex viscosity of PP, PP/CA, PPS nanocomposites at different frequencies. The test temperature was 190 °C.

heterogeneous nucleation sites during PP extrusion foaming. As Figure 3 shows, the introduction of 0.5–1.0 wt % silica significantly increased the cell density of PP from 10^{4-5} to 10^{8-9} cells/cm³, and increased the expansion ratio from 1.5 to 12.6 to 2.7–19.5. To the best of our knowledge, this kind of improvement in linear PP foamability has never been reported with regard to the addition of other nanofillers, such as nanoclay, in the PP extrusion foaming process. Given that different PP, CA, and CA contents were used in our study,¹¹ however, we could not claim that silica exhibited a higher efficiency in inducing cell nucleation compared with clay during PP extrusion foaming, and further research is needed.

In the polymer/filler nanocomposite foaming systems, the dispersion of nanofiller and nanofiller content are critical parameters in determining the cell morphology of the final foamed samples.^{28–30} Figure 1 shows that plentiful well-dispersed multi-silica aggregates were present in PPS5.0. The masterbatch dilution process did not further disperse or aggregate the silica particles. An increase in silica content tended to increase the number of aggregates. A clear increase in the cell density of PPS foams was verified by increasing the silica content from 0.5 to 1.0 wt %, and this contributed to the increase in heterogeneous nucleation sites. At a higher silica content, however, the cell densities of PPS foams tended to decrease even though more heterogeneous nucleation sites were supplied.

Effect of Silica Addition on Cell Coalescence. Poor cell morphology has often been observed in linear PP foams. This was attributed to the low melt strength of the PP resin. It is well-established that the introduction of well-dispersed nanoparticles with high L/D, such as nanoclay, can increase the polymer's melt strength or induce strain hardening in the melt.^{4–6} Cell growth is a biaxial extension to the cell walls in nature, and the nanoclay introduction has been thought to stabilize cell structure and reduce cell coalescence during the foam processing.^{9,11} Figure 6 shows the complex viscosity of PP, PP/CA, and PPS at different frequencies, where the test temperature was 190 °C. With PP, no Newtonian plateau was observed at low frequencies, and a shearing thinning behavior was present at high frequencies. The addition of CA with a high MFI tends to decrease the viscosity of the PP/CA gradually, but the frequency dependency of viscosity on them does not change very much. When nanosilica is introduced into the PP/CA, it is seen that the melt viscosity of

the PPS increases slightly. Similar results have been observed in PP/CA/silica nanocomposite systems,³¹ where the introduction of 5.0 wt % silica only slightly increased the melt viscosity of the PP/CA.

The increase of the viscosities of polymer/filler nanocomposites is generally attributed to the percolated networks caused by the physical interaction of nanofillers. In the case of nanofiller with a long L/D ratio, such as nanoclay, the percolation threshold is quite low. This is because the anisotropy of the tactoids and the individual layers prevent free-rotation of these elements, and thus, dissipate the stresses in the polymer melt.³² In the case of a nanofiller with a low L/D ratio, such as silica, however, the percolation threshold is quite high, and low silica is supposed to exhibit low physical interaction because of the long distance between two particles.³¹ Therefore, it is believed that silica's isotropic shape is the main reason for the weak effect of the silica addition on the melt viscosity of PP. The presence of high-MFI CA was expected to decrease the melt viscosity of the PP/CA. Its negative effect on the melt viscosity was greater than the positive effect of the silica addition, and yielded the decrease of melt viscosity in the PPS nanocomposites. At a high silica content, high CA content further decreased the melt viscosity of the PPS nanocomposites.

The presence of a large amount of CA with an MFI of 360 g/10 min seemed to worsen the foaming behavior of PPS. As shown in Figure 2, PPS2.0 and PPS5.0 foams exhibited very poor cell morphology and low cell density at die temperatures of 145 and 145–140 °C, respectively, while other foams with low CA content presented good cell morphologies and a much higher cell densities, even though the high silica content of PPS2.0 and PPS5.0 could provide more heterogeneous nucleating sites during foaming. The effect of nanofiller content on the cell morphology of foams is usually associated with the dispersion of nanofillers in the polymer matrix.²⁹ Normally, the improved nanofiller dispersion tends to increase heterogeneous nucleation sites, and hence enhances cell nucleation. On the other hand, good nanofiller dispersion is usually easily achieved at a low nanofiller loading. It tends to exhibit a more obvious effect on the viscoelastic properties of the polymer melt than does poor dispersion,⁵ and thus suppresses cell coalescence. Both cases usually lead to a presence of optimum nanofiller content that result in the best foam cell morphology.²⁸ In this study, however, silica did not obviously redisperse or further aggregate during dilution processing, and PPS nanocomposites with a higher silica content tended to have higher heterogeneous nucleating sites. Considering the decreased cell density of the PPS5.0 foams, it was believed that a large number of nucleated bubbles could not survive, and serious cell coalescence did occur during the PPS5.0 foaming process.

PPS nanocomposites with high silica content was associated with high CA content in this study, and the presence of a large amount of CA could be a main reason why PPS5.0 exhibited poor foaming behavior even it potentially possessed high heterogeneous nucleation sites. The CA had a very low viscosity, i.e. 360 g/10 min, as shown in Figure 6, the introduction of CA tended to significantly reduce the viscosities of PPS nanocomposites. Low viscosity usually reduces the pressure drop rate at the die exit, which decreases the cell nucleation rate. Moreover, low viscosity is generally accompanied by low melt strength, which facilitates the occurrence of cell coalescence. The presence of serious cell coalescence facilitated quick gas diffusion out of the sample that resulted in a low foam expansion in the PPS5.0

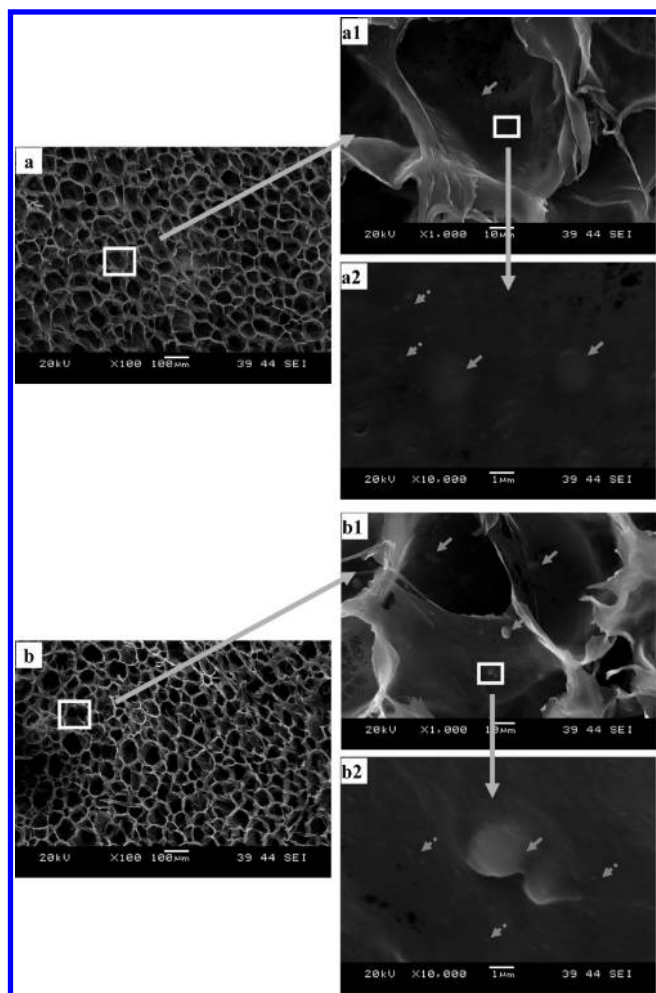


Figure 7. Dispersion of nanosilica, pointed by the dotted arrow, and phase-separated spherical particles, pointed by the arrow, in PPS1.0 (a, a1, and a2) and PPS5.0 (b, b1, and b2) foams.

foams. These results suggested that a suitable match between the CA and the PP should be established to further improve the foaming behavior of PPS with a high silica loading.

Polymeric Foaming Improves Silica Dispersion. Figure 7 shows the SEM micrographs of PPS1.0 and PPS5.0 foams with different magnifications, where the foams were obtained at die temperatures of 135 and 130 °C, respectively. At a low magnification of $\times 100$, PPS nanocomposite foams with uniform cell distribution were observed. At a high magnification of $\times 1000$, several spherical particles sized at about 2–5 μm were found in the cell wall. These types of spherical particles had been observed in unfoamed PP and PPS nanocomposites, which could be composed of the original rubber or CA phases. It is interesting to note that the number and size of spherical particles increased with CA content. This supports the idea that PP and the CA exhibited phase separation at a high CA loading. At a higher magnification of $\times 10000$, a large quantity of multisilica aggregates are visible in the cell wall. Compared with Figure 1, it was interesting to find that the size of silica aggregates clearly decreased and were uniformly dispersed in the polymer matrix.

It is known that the cell growth process results from the extensional flow of the polymer/gas solution, and that the cell walls are biaxially stretched during polymeric foaming.⁸ Given

the interface bonding between the polymer matrix and the nanoparticles, the applied biaxial stretching action during cell growth was expected to transfer from the matrix onto the nanoparticles. This process tended to redisperse the silica in the foamed samples. A similar phenomenon has been reported in other foaming systems, such as polycarbonate/silica³³ and PP/clay¹⁰ nanocomposites. This outcome could provide a novel method by which to disperse nanoparticles in the polymer matrix.

CONCLUSION

In this study, PPS nanocomposite masterbatch were compounded by a twin-screw extruder, and nanocomposites with low silica content were obtained by a dilution process. SEM observation indicated that nanosilica tended to aggregate in the PP matrix, but the multisilica aggregates sized at 80–350 nm could be well dispersed in the PP due to the addition of CA. Meanwhile, it was verified that the dilution process did not affect the dispersion the multisilica aggregates. PP and PPS nanocomposites were foamed using a continuous extrusion foaming system with 5 wt % CO_2 as a physical blowing agent. As expected, PP exhibited poor foaming behavior due to poor cell nucleation as well as cell coalescence, where the cell density was low at 10^{4-5} cells/ cm^3 and the cell structure was nonuniform. Decreased die temperature tended to improve the cell morphology of the PP foams slightly. The introduction of small amounts of nanosilica, that is, 0.5 and 1.0 wt %, dramatically improved the foaming behavior of the PP. The resultant PPS nanocomposite foams presented uniform cell structure dispersion and significantly increased both cell density (10^{8-9} cells/ cm^3) and foam expansion (up to 19.5). Moreover, the presence of nanosilica also clearly broadened the foaming window of the PP. The foaming behavior of the PPS2.0 and PPS5.0 nanocomposites were poor, where the cell coalescence was observed at higher die temperature and the foam expansion ratio decreased dramatically, even though high silica content could supply increased heterogeneous nucleation sites. The melt viscoelastic results demonstrated that the addition of a large amount of low viscosity CA reduced the overall melt viscosity. The effect of the foaming process on the dispersion of nanosilica was also studied. It was found that multisilica aggregates could be dispersed during the foaming process. This was caused by the applied biaxial stretching action during cell growth that had been expected to transfer onto the nanoparticles.

AUTHOR INFORMATION

Corresponding Author

*E-mail: park@mie.utoronto.ca.

ACKNOWLEDGMENT

The authors are grateful to the National Natural Science Foundation of China (Grants 51003115) and the Natural Sciences and Engineering Research Council of Canada (NSERC) for their financial support of this study.

REFERENCES

- (1) Burt, J. G. The Elements of Expansion of Thermoplastics Part II. *J. Cell. Plast.* **1978**, *14*, 341.

- (2) Park, C. B.; Cheung, L. K. A Study of Cell Nucleation in the Extrusion of Polypropylene Foams. *Polym. Eng. Sci.* **1997**, *37*, 1.
- (3) Zhai, W. T.; Wang, H. Y.; Yu, J.; Dong, J. Y.; He, J. S. Cell Coalescence Suppressed by Crosslinking Structure in Polypropylene Microcellular Foaming. *Polym. Eng. Sci.* **2008**, *48*, 1312.
- (4) Okamoto, M.; Nam, P. H.; Maiti, P.; Kptaka, T.; Hasegawa, N.; Usuki, A. A House of Cards Structure in Polypropylene/Clay Nanocomposites Under Elongational Flow. *Nano Lett.* **2001**, *1*, 295.
- (5) Park, J. U.; Kim, J. L.; Kim, D. H.; Ahn, K. H.; Lee, S. J. Rheological Behavior of Polymer/Layered Silicate Nanocomposites under Uniaxial Extensional Flow. *Macromol. Res.* **2006**, *14*, 318.
- (6) Koo, C. M.; Kim, J. H.; Wang, K. H.; Chung, I. J. Melt-Extensional Properties and Orientation Behaviors of Polypropylene-Layered Silicate Nanocomposites. *J. Polym. Sci., Part B: Polym. Phys.* **2005**, *43*, 158.
- (7) Werner, P.; Verdejo, R.; Wöllecke, F.; Altstädt, V.; Sandler, J. K. W.; Shaffer, M. S. P. Carbon Nanofibers Allow Foaming of Semicrystalline Poly(ether ether ketone). *Adv. Mater.* **2005**, *17*, 2864.
- (8) Stange, J.; Münstedt, H. Rheological Properties and Foaming Behavior of Polypropylenes with Different Molecular Structures. *J. Rheol.* **2006**, *50*, 907.
- (9) Okamoto, M.; Nam, P. H.; Maiti, P.; Kotaka, T.; Nakayama, T.; Takada, M.; Ohsima, M.; Usuki, A.; Hasegawa, N.; Okamoto, H. Biaxial Flow-Induced Alignment of Silicate Layers in Polypropylene/Clay Nanocomposite Foam. *Nano Lett.* **2001**, *1*, 503.
- (10) Zheng, W. G.; Lee, Y. H.; Park, C. B. Use of Nanoparticles for Improving the Foaming Behaviors of Linear PP. *J. Appl. Polym. Sci.* **2010**, *117*, 2972.
- (11) Zhai, W. T.; Kuboki, T.; Wang, L.; Park, C. B.; Lee, E. K.; Naguib, H. E. Cell Structure Evolution and the Crystallization Behavior of PP/Clay Nanocomposites Foams Blown in Continuous Extrusion. *Ind. Eng. Chem. Res.* **2010**, *49*, 9834.
- (12) Naguib, H. E.; Park, C. B.; Panzer, U.; Reichelt, N. Strategies for Achieving Ultra-low-Density PP Foams. *Polym. Eng. Sci.* **2002**, *42*, 1481.
- (13) Reichelt, N.; Stadlbauer, M.; Folland, R.; Park, C. B.; Wang, J. PP-Blends with Tailored Foamability and Mechanical Properties. *Cell. Polym.* **2003**, *22*, 315.
- (14) Lee, E. K.; Lee, K. M.; Jung, P. U.; Naguib, H. E.; Park, C. B. Comparison of Random and Block Polypropylene Copolymers in Extrusion Foaming. *SPE ANTEC Tech. Pap.* **2009**, Paper No. 1021.
- (15) Wunderlich, B. *Macromolecular Physics, Crystal Structure, Morphology, Defects*; Academic Press: New York, 1973, Vol. 1.
- (16) Bikiaris, D. N.; Vassiliou, A.; Pavlidou, E.; Karayannidis, G. P. Compatibilisation Effect of PP-g-MA Copolymer on IPP/SiO₂ Nanocomposites Prepared by Melt Mixing. *Eur. Polym. J.* **2005**, *41*, 1965.
- (17) Lee, S. H.; Kontopoulou, M.; Park, C. B. Effect of Nanosilica on the Co-continuous Morphology of Polypropylene/Polyolefin Elastomer Blends. *Polymer* **2010**, *51*, 1147.
- (18) González-Montiel, A.; Keskkula, H.; Paul, D. J. Morphology of Nylon 6/Polypropylene Blends Compatibilized with Maleated Polypropylene. *J. Polym. Sci. Part: B Polym. Phys.* **1995**, *33*, 1751.
- (19) Zheng, W. G.; Lee, Y. H.; Park, C. B. The Effects of Exfoliated Nano-clay on the Extrusion Microcellular Foaming of Amorphous and Crystalline Nylon. *J. Cell. Plast.* **2006**, *42*, 271.
- (20) Lee, Y. H.; Kuboki, T.; Park, C. B.; Sain, M. The Effects of Nanoclay on the Extrusion Foaming of Wood Fiber/Polyethylene Nanocomposites. *Polym. Eng. Sci.* **2010** accepted.
- (21) Guo, G.; Wang, K. H.; Park, C. B.; Kim, Y. S.; Li, G. Effects of Nanoparticles on Density Reduction and Cell Morphology of Extruded Metallocene Polyethylene/Wood Fiber Nanocomposites. *J. Appl. Polym. Sci.* **2007**, *104*, 1058.
- (22) Colton, J. S.; Suh, N. P. The Nucleation of Microcellular Thermoplastic Foam with Additives: Part I: Theoretical Considerations. *Polym. Eng. Sci.* **1987**, *27*, 485.
- (23) Wang, C.; Leung, S. N.; Bussmann, M.; Zhai, W. T.; Park, C. B. Numerical Investigation of Nucleating Agent-Enhanced Heterogeneous Nucleation, *Ind. Eng. Chem. Res.* **2010**, *49*, 12783.
- (24) Wang, L. C.; Leung, S. N.; Bussmann, M.; Park, C. B. How Do Multiple Flights Improve the Effectiveness of a Cooling Extruder Screw? *SPE ANTEC Tech. Pap.* **2010**, Paper No. 1037.
- (25) McClurg, R. B. Design Criteria for Ideal Foam Nucleating Agents. *Chem. Eng. Sci.* **2004**, *59*, 5779.
- (26) Spital, P.; Macosko, C. W.; McClurg, R. B. Block Copolymer Micelles for Nucleation of Microcellular Thermoplastic Foams. *Macromolecules* **2004**, *37*, 6874.
- (27) Dogan, A. U.; Dogan, M.; Onal, M.; Sarikaya, Y.; Aburub, A.; Wurster, D. E. Baseline Studies of the Clay Minerals Society Source Clays: Specific Surface Area by the Brunauer Emmett Teller (BET) Method. *Clays Clay Miner.* **2006**, *54*, 62.
- (28) Lee, Y. H.; Wang, K. H.; Park, C. B.; Sain, M. Effects of Clay Dispersion on the Foam Morphology of LDPE/Clay Nanocomposites. *J. Appl. Polym. Sci.* **2007**, *103*, 2129.
- (29) Zeng, C. C.; Han, X. M.; Lee, L. J.; Koelling, K. W.; Tomasho, D. L. Polymer-Clay Nanocomposite Foams Prepared Using Carbon Dioxide. *Adv. Mater.* **2003**, *15*, 1743.
- (30) Shen, J.; Zeng, C. C.; Lee, L. J. Synthesis of Polystyrene-Carbon Nanofibers Nanocomposite Foams. *Polymer* **2005**, *46*, 5218.
- (31) Liu, Y.; Kontopoulou, M. The Structure and Physical Properties of Polypropylene and Thermoplastic Olefin Nanocomposites Containing Nanosilica. *Polymer* **2006**, *47*, 7731.
- (32) Kim, D. H.; Fasulo, P. D.; Rodgers, W. R.; Paul, D. R. Effect of the Ratio of Maleated Polypropylene to Organoclay on the Structure and Properties of TPO-Based Nanocomposites. Part I: Morphology and Mechanical Properties. *Polymer* **2007**, *48*, 5960.
- (33) Zhai, W. T.; Yu, J.; Wu, L. C.; Ma, W. M.; He, J. S. Heterogeneous Nucleation Uniformizing Cell Size Distribution in Microcellular Nanocomposites Foams. *Polymer* **2006**, *47*, 7580.